Energy Equip. Sys./ Vol. 8/No. 1/March 2020/ 81-90

ENERGY EQUIPSYS

Energy Equipment and Systems

http://energyequipsys.ut.ac.ir
www.energyequipsys.com

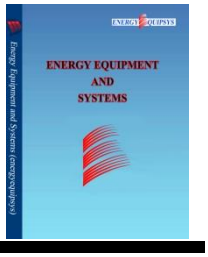

Power optimization of a piezoelectric-based energy harvesting cantilever beam using surrogate model

Authors

Arman Mohammadi [a]
Pooyan Nayyeri [a]
Mohammad Reza Zakerzadeh [a*]
Farzad AyatollahzadehShirazi [a]

[a] School of Mechanical Engineering, College of Engineering, University of Tehran, Iran

Article history:

Received : 22 June 2019
Accepted : 20 September 2019

ABSTRACT

Energy harvesting is a conventional method to collect the dissipated energy of a system. In this paper, we investigate the optimal location of a piezoelectric element to harvest maximum power concerning different excitation frequencies of a vibrating cantilever beam. The cantilever beam oscillates by a concentrated sinusoidal tip force, and a piezoelectric patch is integrated on the beam to generate electrical energy. To this end, the system is modeled with analytical governing equations, then a Deep Neural Network (DNN)-based surrogate model is developed to appropriately model the system within the range of its first three natural frequencies. The surrogate model has significantly abated the computation cost. Thus, the optimization time is reduced drastically. Our investigations led to an optimal piezoelectric location for different excitation frequencies, which can result in maximum electrical output power. This location is highly dependent on the excitation frequency. When excitation frequency equals to natural frequencies, the maximum harvested power increases considerably.

Keywords: Cantilever Beam, Piezoelectric, Surrogate Model, Deep Neural Network, Energy Optimization.

1. Introduction

One of the serious deficiencies in self-governing systems is their deprivation of sustainable energy supplies. In today's electrical devices, usage of electrical energy for running electrical circuits has been reduced drastically. Therefore the importance of electrical power harvesting from environmental elements has increased. The use of piezoelectric materials as an energy harvesting element in flexible structures has been of popular concern in recent years. The main advantages of piezoelectrics are simple and effective integration with structures, low economic cost, and high precision in high duty cycles. On the other hand, cantilever beams are a modest modeling simplification for the vibration of many engineering cases like robot arms, airfoils, etc. To convert mechanical vibration energy into electrical power, some methods have been proposed; specifically, piezoelectric, electromagnetic, and electrostatic devices can perform this energy transformation [1, 2]. At the same time, the research about smart structures with piezoelectric elements has been studied extensively in recent years. Moreover, plenty of review articles about energy conversion in smart structures have been published [3, 4].

To attain the proper view of the behavior of smart structures in different vibration situations, some general methods for modeling the

* Corresponding author: Mohammad Reza Zakerzadeh
School of Mechanical Engineering, College of Engineering, University of Tehran, Iran
Email: zakerzadeh@ut.ac.ir

vibration of smart structures have been proposed. Some models are based on the finite element method [5, 6]. Despite the finite element's efficient method, analytical solutions have attracted more interests in energy-based studies, because of their straightforward nature in deriving general governing equations of motion [7].

To increase the generated power of harvesting devices, some optimization methods have been conducted. In [8, 9] the optimum structure of a beam for maximum harvested energy has been investigated. In the case of the vibrating base, some advance studies have been made. In [10, 11] experimental and numerical research has been done on the generated voltage induced by vibrations of a cantilever beam in different frequencies close to the first natural frequency of the cantilever beam. Also, the topology of applied piezoelectric has been optimized in [12]. Some extension on the simple cantilever beams has been performed by attaching a tip mass to the free end, and then the harvested electrical power has been examined on the shunted circuit by changing the weight of the tip mass [13, 14].

The Finite Element (FE) approach for optimization would lead to time consuming and expensive calculations. Despite this disadvantage, Park, J. et al. have designed an optimization procedure to reduce the cost of computation required for the optimization of the shape of a cantilever beam by the FE method [15]. Here, to reduce intensive computations of the analytical model of a smart piezoelectric-based cantilever beam, a surrogate model or meta-model has been used. Perera A. et al. [16] have shown that surrogate models based on Artificial Neural Networks (ANN) can reduce computation time up to 84% and can catalyst the optimization process drastically. Also, hybrid optimization algorithms can be used to maintain optimization accuracy. Surrogate models, coupled with numerical optimization heuristics, were widely used in agricultural [17], chemical [18], and mechanical [19-21] engineering fields. On the other hand, Villarrubia G. et al. have proposed a neural network-based optimization method, enabling us to find the derivative of the approximated function [22].

In this paper, first, the governing equation of a piezoelectric-based energy harvesting system is developed. To obtain the maximum harvested power from the cantilever beam smart structure in different excitation frequencies, the location of the piezoelectric on the cantilever beam is optimized. Also, to reduce the drastic computation cost in the optimization process, a surrogate model is developed. Finally, optimization results are presented to illustrate the effect of the optimum location of piezoelectric on the harvested power as well as on the system efficiency.

2. General Modeling of Piezoelectric/Beam Equation

Figure 1 illustrates the schematic view of a piezoelectric integrated cantilever beam. As can be seen, the forced vibration is streaming the electrical flow into the shunted circuit.

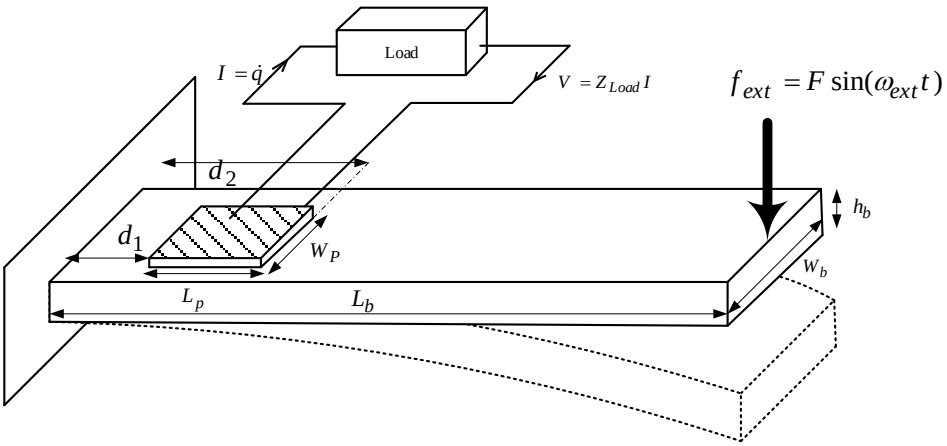

Fig.1. Induced current into energy harvesting equation of piezoelectric

The first step in acquiring the general relation between the motion of the cantilever beam and the induced voltage in the piezoelectric patch is to derive the governing equations of the system. Eq. (1) shows the Hamilton principle,

$$\delta H = \delta \int_{t_1}^{t_2} (T - U + W)dt = 0 \tag{1}$$

where, T and U are the kinetic energy and potential energy, respectively, while W is the virtual work of external forces applied on the system. In order to extract the energy parameters of Eq. (1) [23], the fundamental equations of piezoelectric actuator and sensors are needed:

Actuator equation:

$$M\ddot{w} + C\dot{w} + Kw = f_{ext} + \theta V_{sh} \tag{2}$$

Sensor equation:

$$Q = \theta^T w + C_p V_{sh} \tag{3}$$

It should be noticed that w is the lateral deflection of the beam and M, C and K are the mass, damping and stiffness matrices of the piezo/beam system, respectively. Also, Q is the piezoelectric charge and θ and is the electromechanical coupling matrix. Notice that C_p, V_{sh} are the capacitance and induced voltage in the piezoelectric, respectively. The constitutive equation for the piezoelectric element in one of its common form is presented in Eq. (4) [24]:

$$\begin{bmatrix}\sigma \\ E\end{bmatrix} = \begin{bmatrix}E_s & -h \\ -h & \beta\end{bmatrix}\begin{bmatrix}\epsilon \\ D\end{bmatrix} \tag{4}$$

where, σ and E are stress and electric field in the piezoelectric, respectively. E_s is the elastic modulus at the constant displacement, h is the piezoelectric constant and β is dielectric constant. Now with a basic knowledge about the piezoelectric and beam, parameters in Eq. (2) can be calculated. Consider that the kinetic and potential energy in the system consist of two terms, the beam and the piezoelectric part; first of all, the kinetic energy is defined by Eq. (5) [25].

$$T = T_b + T_p\,,$$
$$T_b = \frac{1}{2}\int_0^{L_b} \rho_b A_b \left(\frac{\partial w}{\partial t}\right)^2 dx\,,$$
$$T_p = \frac{1}{2}\int_{d_1}^{d_2} \rho_p A_p \left(\frac{\partial w}{\partial t}\right)^2 dx \tag{5}$$

The strain energy of the piezo/beam system can be described in Eq. (6). Note that the potential energy of the piezoelectric consists of two parts; the dynamics of the system and the electromechanical property of the piezo material.

$$U = U_b + U_p\,,$$
$$U_b = \frac{1}{2}\int_0^{L_b} E_b I_b \left(\frac{\partial^2 w}{\partial t^2}\right)^2 dx\,,$$
$$U_p = \frac{1}{2}\int_V (\epsilon^T \sigma + ED)dV = \frac{1}{2}\int_{d_1}^{d_2} (E_p I_P + 2bh_{31}Dz_n\left(\frac{\partial^2 w}{\partial x^2}\right) + A_p\beta_{33}D^2)dx \tag{6}$$

The virtual work of Hamilton's principle consists of three parts; the first part is induced by piezoelectric voltage, the second part is from the external force on the cantilever beam, and the last part is generated from internal damping of the beam, as shown in the following equation:

$$\delta W = Z\dot{Q}\delta Q + \int_0^{L_b} f(x,t)\delta w - \int_0^{Lb} C_b \frac{\partial w}{\partial t}\delta w dx \tag{7}$$

where, Z is the overall impedance of the circuit, including the piezoelectric. Now, by using the assumed mode method, the Eq. (2) can be converted into a set of ordinary differential equations by using the following approximation.

$$w(x,t) = \sum_{i=1}^{n} \psi_i(x) W_i(t) = [\psi]^T [W] \tag{8}$$

In the above equation, ψ_i is the mode shape of the cantilever beam which is selected as [26]:

$$\psi_i(x) = cosh\beta_i x - cos\beta_i x - \sigma_i(sinh\beta_i x - sin\beta_i x) \tag{9}$$

Applying these mode shapes into the Hamilton equation, the following general equation of motion would be generated:

$$M\ddot{W}(t) + C_b\dot{W}(t) + KW(t) = f_{ext} + f_{piezo} \quad (10)$$

where,

$$M = \rho_b A_b \int_0^{L_b} \psi_i \psi_i^T dx + \rho_p A_p \int_{d_1}^{d_2} \psi_i \psi_i^T dx$$

$$K = E_b I_b \int_0^{L_b} \psi_i'' \psi_i''^T dx + E_p I_p \int_{d_1}^{d_2} \psi_i'' \psi_i''^T dx$$

$$C = \alpha M + \beta K$$

$$f_{ext} = \int_0^{L_b} \psi_i f(x,t) dx$$

$$f_{piezo} = -b_p h_{31} E_p V_L h_p (h_b + h_p)[\psi_i'(d_2) - \psi_i'(d_1)]$$

It should be mentioned that in order to extract the damping matrix, Rayleigh-Ritz method has been used [27]:

$$\begin{cases} \alpha + \beta\omega_{n_1}^2 - 2\zeta_1\omega_{n_1} = 0 \\ \alpha + \beta\omega_{n_2}^2 - 2\zeta_2\omega_{n_2} = 0 \end{cases} \quad (11)$$

The coefficients ζ_1, ζ_2 in Eq. (11) are determined through experimental tests. In order to calculate the induced voltage of the piezoelectric, the governing equation of the circuit, including the piezoelectric sensor, should be used.

3. General Modeling of Piezoelectric Energy Harvesting Circuit

The current equation can be obtained by differentiating Eq. (3) and then substituting it into the voltage equation of the circuit shown in Fig. 1. As a result, we can define the circuit model as Eq. (12):

$$V_L = -ZI = -Z\left(\frac{d}{dt}([d]^T\{T\} + [\varepsilon]^T\{E\})\right) \quad (12)$$

By using Laplace operator on the governing equation of the circuit, the equations will be transferred into the linear space. Also, by substituting the mode shapes of the cantilever beam into the variables, the redefined voltage of the piezoelectric would be as follows [24]:

$$V_L = \frac{-ZC_0D_nsW}{1 + ZC_ps} \quad (13)$$

where,

$$C_0 = d_{31}E_p^E b_p\left(\frac{h_p}{2} + h_p\right) \text{ and } D_n = \int_{d_1}^{d_2} \frac{\partial^2\psi_i}{\partial x^2} dx \quad (14)$$

In order to achieve the electrical power attained from the induced voltage of piezoelectric, the average power is determined from the following equation:

$$P_{ave} = \frac{{V_{rms}}^2}{Z} \quad , \quad V_{rms} = \frac{V}{\sqrt{2}} \quad (15)$$

4. Surrogate Model

Surrogate models are widely used to decrease the complexity and computation cost of the analytical models. A surrogate model can be modeled in different ways. We have used Artificial Neural Networks (ANN) to train a deep neural network to mimic the analytical model behavior. In the optimization process, we will use the developed surrogate model to find optimum points of an objective function due to different excitation frequencies. This approach enables us to use numerical optimization heuristics (e.g. Genetic Algorithm) to find the optimal points.

To obtain the proper surrogate model, the system was modeled by its first three mode shapes. The natural frequencies of the system were determined by solving the eigenvalue problem of Eq. (10), which were found to be 3.49, 21.72, and 60.62 Hz. In the following section, our model was trained with a dataset acquired by applying a sinusoidal excitation force with a frequency range of 0 to 64 Hz to contain the dynamic behavior of the system for the three mode shapes.

4.1. Artificial Neural Network (ANN)

An Artificial Neural Network (ANN) consists of artificial neurons with specific activation functions. A perceptron is a simple neuron with the activation function presented in (16):

$$f(x) = \begin{cases} 1 & ,x > 0 \\ 0 & ,x \leq 0 \end{cases} \quad (16)$$

A simple ANN can consist of several perceptrons in a feedforward arrangement to create a multilayer perceptron (MLP). MLPs have at least three layers: an input layer, a hidden layer, and an output layer. However, in an MLP, some neurons can possess nonlinear activation functions such as (17) and (18), which is called hyperbolic tangent and logistic sigmoid functions, respectively.

$$\tanh(x) = \frac{e^{x} - e^{-x}}{e^{x} + e^{-x}} \quad (17)$$

$$\text{logsig}(x) = \frac{1}{1 + e^{-x}} \quad (18)$$

As we can deduce, “tanh” and “logsig” functions range from -1 to 1 and 0 to 1, respectively. This is useful when we are modeling different analytical models, because some physical parameters cannot be a negative value, inherently.

4.2. Deep Neural Networks (DNN)

An ANN with more than one hidden layer is occasionally called Deep Neural Networks (DNN). While MLPs are good at classification and curve fitting, a DNN can learn more complex functions, due to more connections between neurons and the higher number of neurons and hidden layers. DNNs use more complicated activation functions and more sophisticated neuron types [28].

4.3. Trained Model

After a concise introduction about ANNs, we are ready to train a DNN to faithfully present the obtained analytical model for the piezoelectric-based cantilever beam energy harvester. To this end, we have used two input variables; excitation frequency and piezoelectric location, and one output; power generated by the piezoelectric to train the DNN model. By using the trial and error approach, a two-layer neural network was obtained as shown in Fig.2. The first hidden layer consists of 20 neurons with tanh activation function, while the second hidden layer has only 10 neurons with logsig activation function. The activation function of output neuron is a linear function that passes the sum of all weighted inputs as output.

Levenberg-Marquardt backpropagation method was implemented to update the weights and bias of each neuron to obtain a decent result [29]. The DNN was trained with the calculated dataset containing more than 5000 exclusive data from the analytical model. The training, validation, and test datasets were selected randomly with ratios of 70%, 15%, and 15% of the total dataset, respectively. While obtaining 5000 data from the analytical model can take about 21 hours for computation by a typical computer, procuring the same amount of data using the trained DNN can only take about 70 seconds. As a result, the computation time has drastically reduced, which enables us to use numerical optimization approaches. Without the implementation of the surrogate model, we could optimize the objective function by neither numerical methods nor exact methods at a normal time.

Figure 3 shows the surface obtained by the two approaches. As it can be seen, the trained DNN could properly mimic the original analytical model. Specifically, the DNN completed training in 211 iterations with the mean square error of 3.71e-15. In the next section we will use the DNN in the optimization process.

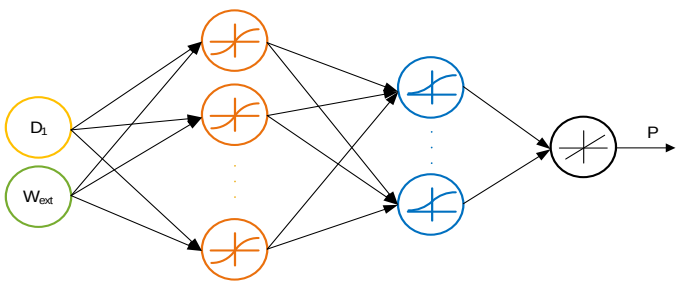

Fig.2. Deep neural network architecture used as a surrogate model.

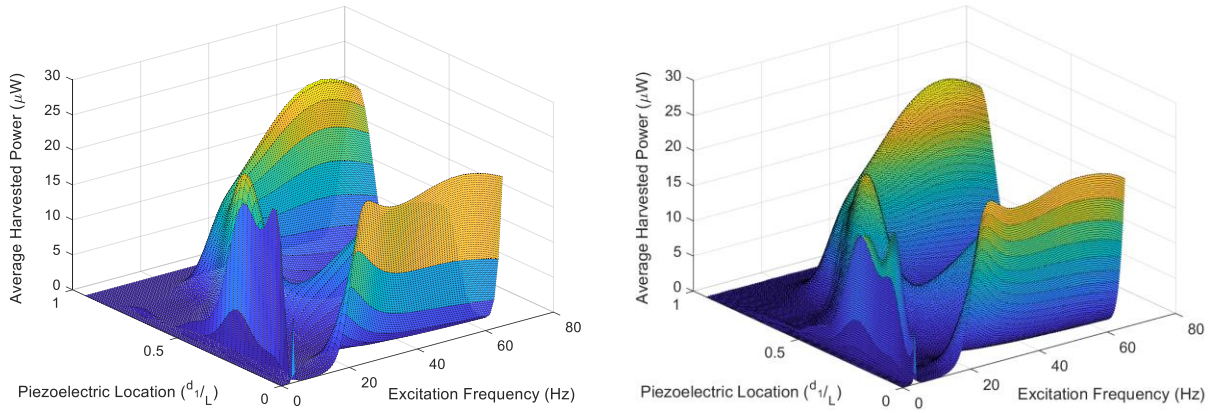

Fig. 3. The effect of excitation frequency and piezoelecteric location on the average power harvested from piezoelectric. a)results from the analytical model. b)results from the trained DNN

5. Optimization

Our primary goal in this section is to find optimum locations of the piezoelectric on the cantilever beam to maximize the harvested energy for different excitation frequencies. According to the intense computation of the analytical governing equations, we have developed a surrogate model in the previous section. In this section, the surrogate model and Genetic Algorithm (GA) are used to optimize the harvested energy by the system. The genetic algorithm was implemented with a population of 50, crossover fraction of 0.8, and Gaussian mutation with scale and shrink of 1.0. We have used excitation frequencies ranging between 0 to 64 Hz (400 rad/s). For each frequency, the optimization was done with 30 iterations to find the optimum point. An overview of optimal piezoelectric locations is illustrated in Fig.4. It is obvious that by getting close to each natural frequencies, the optimum location for the maximum efficient energy harvesting process transits to the antinodes (middle of the nodes) of the resonated mode shape.

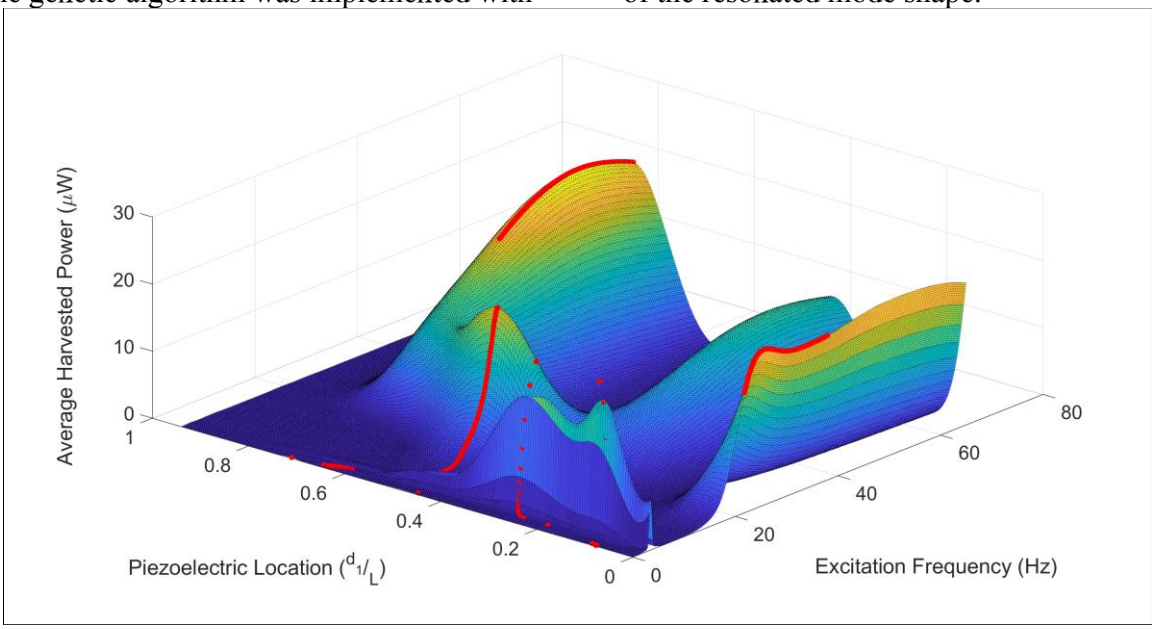

Fig.4. Optimum points for dimensionless piezoelectric location in different excitation frequencies to obtain maximum average harvested power

6. Results and Discussions

The properties of the beam and the piezoelectric are presented in Table 1 and Table 2, respectively. The analytical model of the cantilever beam was introduced in previous sections. Also the proper model for the induced voltage and the harvested power have been developed with the first three vibration natural frequencies. As a matter of computational cost, the surrogate model for this process have been proposed. The optimum location for piezoelectric energy harvester depends drastically on the excitation frequency. Figure 5 demonstrates the three natural frequencies of the beam and their corresponding maximum average harvested power. The solid red curve indicates the average harvested power and a solid blue curve with square markers shows the mode shapes of the beam in the corresponding natural frequencies. As we expected, the optimal location of the piezoelectric element highly depends on the working frequency, which is majorly determined with the dominant natural frequency. A mathematical explanation of this phenomena is that the induced voltage of piezoelectric depends on the integration of changes in the slope of the beam, according to Eq. (13). By increasing the excitation frequency, the higher mode shapes gain a higher portion to the overall shape. Thus, by integrating of the curvature of the beam, which is a symbol of slope changes, the direct relation can be observed between optimal piezoelectric location and beam dominant mode shape antinodes (the section with the highest curvature).

The overall power generated by the piezo element as a result of the vibration of the structure is incremented with increasing the excitation frequency of the applied force, as it is illustrated in Fig.6.The local extrema (around 3 Hz, 20 Hz, and 60 Hz) are due to resonance phenomena in the structure.

7. Conclusions

The main struggle in energy harvesting studies is to achieve the best performance of transducers.

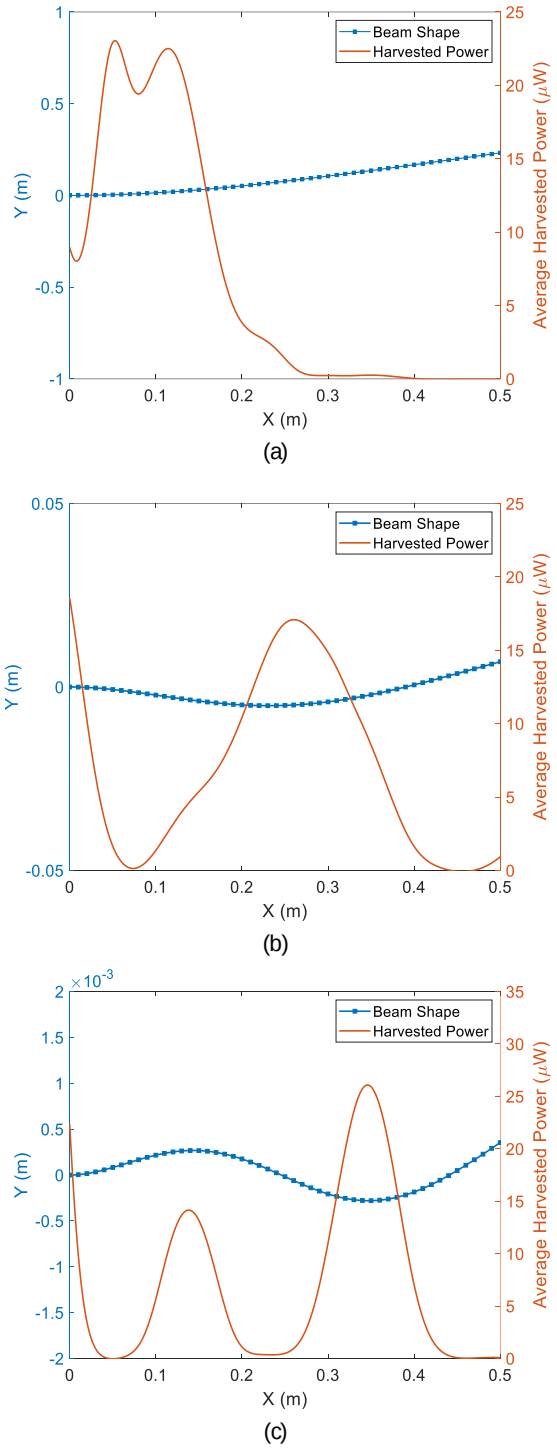

Fig.5. Average harvested power from piezoelectric in the frist three natural frequencies of the system. (a) excitation frequency of 3.5 Hz, (b) excitation frequency of 22 Hz, (c) excitation frequency of 61 Hz.

Table 1. Beam Properties

Symbol	Quantity	Unit	Value
L_b	Length of the beam	mm	500
W_b	Width of the beam	mm	53.7
h_b	Thickness of the beam	mm	1
ρ_b	The density of the beam	kg/m^3	2690
E_b	Young modulus of the beam	GPa	70.9

Table 2. Piezoelectric Properties

Symbol	Quantity	Unit	Value
$L_p * W_p * h_p$	Dimensions of piezo patch	mm	30*33.27*1
d_{31}	Strain coefficient of piezo patch	C/N	274 E-12
ρ_P	The density of piezo patch	kg/m^3	7750
E_P	Modulus of elasticity of piezo patch	GPa	63.9
C_P	The capacitance of piezo patch	μF	5 E-4

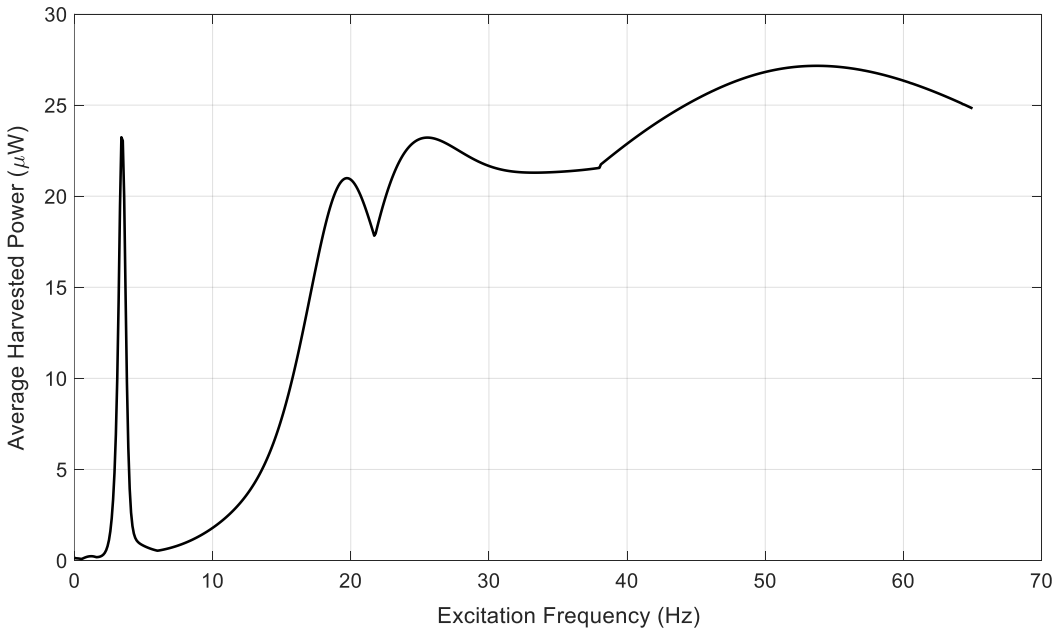

Fig.6. Maximum average harvested power in different excitation frequency of the cantilever beam

Piezoelectric-based energy harvesting structures were optimized in various aspects during previous works. In this paper, the effect of piezoelectric location on the harvested energy for different working frequencies of a cantilever beam has been investigated. To obtain the proper model of the system, the energy-based modeling of the piezo/beam system has been accomplished. On the other hand, because of the complexity of the system equations, a surrogate model was developed to ease the iterative optimization process of the genetic algorithm. The governing equations of the system were obtained by using the first three mode shapes of the system. The optimization process was

performed in a frequency range of 0 to 64 Hz to cover the first three natural frequencies of the system in determining the optimum location of the piezoelectric energy harvester. In the first mode shape, the best location was found to be near the root of the beam; the second and third mode shapes imposed the optimum location to be around the antinodes of the corresponding mode shapes. Also, to gain the most efficient response from the vibration-based energy harvesting systems, this research introduced an effective optimization goal for the location of energy harvester elements and simplified the optimization process.

References

[1] Mitcheson, P.D., et al., MEMS electrostatic micropower generator for low frequency operation. 2004. 115(2-3): p. 523-529.

[2] Williams, C., R.B.J.s. Yates, and a.A. Physical, Analysis of a micro-electric generator for microsystems. 1996. 52(1-3): p. 8-11.

[3] Anton, S.R., H.A.J.S.m. Sodano, and Structures, A review of power harvesting using piezoelectric materials (2003–2006). 2007. 16(3): p. R1.

[4] Cook-Chennault, K.A., et al., Powering MEMS portable devices—a review of non-regenerative and regenerative power supply systems with special emphasis on piezoelectric energy harvesting systems. 2008. 17(4): p. 043001.

[5] Qaisi, M.I.J.A.A., Application of the harmonic balance principle to the nonlinear free vibration of beams. 1993. 40(2): p. 141-151.

[6] Zohoor, H. and F.J.S.I. Kakavand, Vibration of Euler–Bernoulli and Timoshenko beams in large overall motion on flying support using finite element method. 2012. 19(4): p. 1105-1116.

[7] Azrar, L., et al., Semi-analytical approach to the non-linear dynamic response problem of S–S and C–C beams at large vibration amplitudes Part I: general theory and application to the single mode approach to free and forced vibration analysis. 1999. 224(2): p. 183-207.

[8] Jahani, K., M.M. Rafiei, and R. Aghazadeh Ayoubi, Development of a laboratory system to investigate and store electrical energy from the vibrations of a piezoelectric beam %J Energy Equipment and Systems. 2016. 4(2): p. 161-168.

[9] Mateu, L., F.J.J.o.I.M.S. Moll, and Structures, Optimum piezoelectric bending beam structures for energy harvesting using shoe inserts. 2005. 16(10): p. 835-845.

[10] Anderson, T.A. and D.W. Sexton. A vibration energy harvesting sensor platform for increased industrial efficiency. In Smart Structures and Materials 2006: Sensors and Smart Structures Technologies for Civil, Mechanical, and Aerospace Systems. 2006. International Society for Optics and Photonics.

[11] Jiang, S., et al., Performance of a piezoelectric bimorph for scavenging vibration energy. 2005. 14(4): p. 769.

[12] de Almeida, B.V., R.J.J.o.A. Pavanello, and C. Mechanics, Topology Optimization of the Thickness Profile of Bimorph Piezoelectric Energy Harvesting Devices. 2019. 5(1): p. 113-127.

[13] Mohammadi, A., et al. Passive vibration control of a cantilever beam using shunted piezoelectric element. in 2017 5th RSI International Conference on Robotics and Mechatronics (ICRoM). 2017. IEEE.

[14] Roundy, S., et al., Improving power output for vibration-based energy scavengers. 2005. 4(1): p. 28-36.

[15] Park, J., et al., Design optimization of piezoelectric energy harvester subject to tip excitation. 2012. 26(1): p. 137-143.

[16] Perera, A., et al., Machine learning methods to assist energy system optimization. 2019. 243: p. 191-205.

[17] Nguyen, T.H., D. Nong, and K.J.E.M. Paustian, Surrogate-based multi-objective optimization of management options for agricultural landscapes using artificial neural networks. 2019. 400: p. 1-13.

[18] Jeon, K., et al., Development of surrogate model using CFD and deep neural networks to optimize gas detector layout. 2019. 36(3): p. 325-332.
[19] Mousavi, S.M. and S.M. Rahnama, Shape optimization of impingement and film cooling holes on a flat plate using a feedforward ANN and GA %J Energy Equipment and Systems. 2018. 6(3): p. 247-259.
[20] Palagi, L., E. Sciubba, and L.J.A.E. Tocci, A neural network approach to the combined multi-objective optimization of the thermodynamic cycle and the radial inflow turbine for Organic Rankine cycle applications. 2019. 237: p. 210-226.
[21] White, D.A., et al., Multiscale topology optimization using neural network surrogate models. 2019. 346: p. 1118-1135.
[22] Villarrubia, G., et al., Artificial neural networks used in optimization problems. 2018. 272: p. 10-16.
[23] Hagood, N.W., et al., Modelling of piezoelectric actuator dynamics for active structural control. 1990. 1(3): p. 327-354.
[24] Meitzler, A., H. Tiersten, and D.J.N.Y.I.-A. Berlincourt, IEEE standard on piezoelectricity: an american national standard. 1988.
[25] Park, C.-H.J.J.o.S. and vibration, Dynamics modelling of beams with shunted piezoelectric elements. 2003. 268(1): p. 115-129.
[26] Inman, D.J., Vibration with control. 2006: Wiley Online Library.
[27] MacDonald, J.J.P.R., Successive approximations by the Rayleigh-Ritz variation method. 1933. 43(10): p. 830.
[28] Bengio, Y.J.F. and t.i.M. Learning, Learning deep architectures for AI. 2009. 2(1): p. 1-127.
[29] Moré, J.J., The Levenberg-Marquardt algorithm: implementation and theory, in Numerical analysis. 1978, Springer. p. 105-116.